# Systematic investigation of the temperature behavior of InAs/InP quantum nanostructure passively mode-locked lasers

K. Klaime[a,*], R. Piron[a], F. Grillot[a,b], M. Dontabactouny[a], S Loualiche[a], A. Le Corre[a] and K. Yvind[c]

[a]Université Européenne de Bretagne, INSA, CNRS FOTON, 20 avenue des buttes de Coesmes, 35708 Rennes Cedex 7, France
[b]Telecom Paristech, Ecole Nationale Supérieure des Télécommunications, CNRS LTCI, 46 rue Barrault, 75013 Paris, France
[c]Department of Photonics Engineering, Technical University of Denmark, Ørsteds Plads, 2800 Kongens Lyngby, Denmark

*KAMIL.KLAIME@INSA-RENNES.FR

## ABSTRACT

This paper aims to investigate the effects of the temperature on the mode-locking capability of two section InAs/InP quantum nanostructure (QN) passively mode locked lasers. Devices are made with multi-layers of self-assembled InAs QN either grown on InP(100) (5 quantum dashes (QDashes) layers) or on InP (311)B (6 quantum dots (QDs) layers). Using an analytical model, the mode-locking stability map is extracted for the two types of QN as a function of optical absorption, cavity length, current density and temperature. We believe that this study is of first importance since it reports for the first time a systematic investigation of the temperature-dependence on the mode-locking properties of InAs/InP QN devices. Beside, a rigorous comparison between QDashes and QDs temperature dependence is proposed through a proper analysis of the mode-locking stability maps. Experimental results also show that under some specific conditions the mode-locking operation can be temperature independent.

**Keywords: Quantum dots, quantum dashes, semiconductor laser, mode-locked laser**

## 1. INTRODUCTION

Monolithic mode-locked lasers (MLLs) are at the center of interest for a large range of photonic applications. Due to their short pulse and high frequency repetition rate, MLLs are well suited for low-cost applications such as high bit rate optical telecommunications or future optical interconnects [1,2]. So far, many results have been obtained with GaAs material on which, QD MLLs have demonstrated very good operating conditions with a lasing wavelength around 1300 nm and over a wide range of temperature [6]. Indeed, due to their ultra-broad gain bandwidth, ultra-fast gain dynamics, and easily saturated gain, QNs are ideal candidates for the realization of semiconductor MLLs with low threshold current densities and high characteristic temperatures. However, it is known that GaAs material system does not easily allow a lasing emission within the C (1525 -1565 nm) and L (1565-1625 nm) bands. However, these operating wavelengths can be reached with InAs/InP QNs single section [3,4] or multi-section devices [5].. Indeed, growing nanostructures on InP by Molecular Beam Epitaxy (MBE) traditionally leads to either InAs QDashes with (001)InP or to QDs with (311)InP. Because diode lasers are supposed to be located either close to the processor or to the power source, an increase of the temperature of the pn junction can drastically affect the laser performance. To this end, it is important to develop uncooled mode-locked lasers that have a wide margin of operation over temperature. In doing so the complexity and the size of the system as well as the power consumption can be reduced, and the cooling elements can be eliminated. The objective of this paper is to investigate the temperature behavior of two section InAs/InP QN passively MLLs emitting within the C and L telecommunication bands. Devices under study contain five InAs QDash (6 InAs QD respectively) layers grown on InP(100) (InP (311)B respectively). At first, gain and loss spectra are extracted with the so-called segmented contact method (SCM) and the corresponding variations are studied as a function of the current density and

Quantum Dots and Nanostructures: Synthesis, Characterization, and Modeling X, edited by Kurt G. Eyink, Diana L. Huffaker, Frank Szmulowicz, Proc. of SPIE Vol. 8634, 863407 · © 2013 SPIE
CCC code: 0277-786X/13/$18 · doi: 10.1117/12.2005244

for various absorber bias voltages and temperature conditions [7]. Measured values are then incorporated into an analytical model [8,9], which is used to predict the mode-locking temperature-dependence. This numerical investigation is conducted for various values of the absorber to gain length ratio ($L_a/L_g$) both for QDashes and QDs. Calculated stability maps show that for QDs (QDashes respectively), 2% (18% respectively) of the ratio $L_a/L_g$ associated to a current density larger than 10 kA/cm$^2$ (7.5 kA/cm$^2$ respectively) can ensure a good mode-locking conditions until 45°C. To this end, the results point out that QDashes offer a much broader stability range over temperature, which is of first importance for the next generation of semiconductor MLLs used in data-com and telecommunication systems

## 2. ANALYTICAL MODEL DESCRIPTION

This study is based on an analytical model recently proposed in [8] for studying the temperature performance of InAs/GaAs passively mode-locked quantum dot lasers. In a previous paper [9], it was shown that the onset of mode-locking can be described as a sinusoidal modulation of its output optical intensity. In addition, it was also pointed out that this modulation can be analyzed through a net-gain modulation phasor approach. In order to take into account the distribution of gain and loss in the semiconductor material, it has been shown that the criteria for ensuring mode-locking can be recasted as [10]:

$$\frac{L_a}{L_g} > \left( \frac{\dfrac{dg}{dJ}}{\dfrac{dg}{dJ}\Big|_{g=0}} \right)^2 \cdot \frac{g}{a} \quad (1)$$

where $L_g$ and $L_a$ are the lengths of the gain and absorber sections while, g is the modal gain related to the gain section, a is the unsaturated absorption in the absorber and, J is the pump current density. The inclusion of the thermal effects into the model allows determining a proper ratio $L_a/L_g$ which gives rise to a laser operation for various temperature conditions.

An additional constraint proposed in [8] and coming from the threshold condition is expressed as follows:

$$\frac{L_a}{L_g} = \frac{g - \alpha_m - \alpha_p}{a + \alpha_m + \alpha_p} \quad (2)$$

with $\alpha_m$ and $\alpha_p$ are the mirror and internal loss coefficients. Equations (1) and (2) can be used to generate the stability maps and to bound the different regions of mode-locking operations for various temperature conditions. In order to plot (1) and (2) as a function of the pump current density J, values of parameters $\alpha_m$, $\alpha_p$ as well as the variation of the modal gain are required. Transmission loss coefficient $\alpha_m$ is simply calculated by using the relation $\alpha_m = 1/L*\ln(1/R)$ with $L=L_a+L_g$ the total cavity length and R the facet's reflectivity of the cleaved mirrors. Considering a 4 mm total cavity length and R=0.32 leads to $\alpha_m = 3$ cm$^{-1}$. As shown in the following, the internal loss $\alpha_p$ and the absorption coefficients are then extracted from the variations of the material absorption with the operating wavelength. Unsaturated absorption is deduced from the difference between the loss coefficient at the lasing wavelength ($a_{max}$) and the internal loss.

## 3. DEVICES AND FABRICATION

The active material of the semiconductor optical amplifier (SOA) contains 5 InAs QDash or 6 InAs QD layers embedded in a 320 nm of $Ga_{0.20}In_{0.80}As_{0.435}P_{0.565}$ (Q1.18 μm) waveguide grown by Gas source MBE using the double cap method [11](Figure 1). The latter consists in growing the 20 nm thick Q1.18 capping layer over the dashes or dots in two steps separated by a growth interruption under arsenic and phosphorus flux to reduce the height of the highest nanostructures and prevent the Ostwald ripening process. The quality improvement of the active material results in an increase of the carrier lifetime from about 700 ps [12] to 1600 ps [13] leading to lower laser threshold current [14, 15]. The fabricated devices consist of Fabry Perot (FP) multi-sections SOA ridge with a 7° inclined guides. The latter are required to prohibit the laser emission by introducing a low optical reflectivity at the semi-conductor/air interface. The width of the ridge is 2 μm and each section is 1mm long. BCB (bisbenzocyclobutene) processing is used for insulation and planarization between contacts. The etching was done until about 100 nm of p type InP is left above the waveguide. The electrical isolation between sections was done by etching through the highly doped contact layers in a 5 μm trench on

top of the ridge. The electrical resistance between sections is measured to be around 50 kΩ that guarantees a high electrical isolation. The electrical series resistance of the device is found to be about 10 Ω.

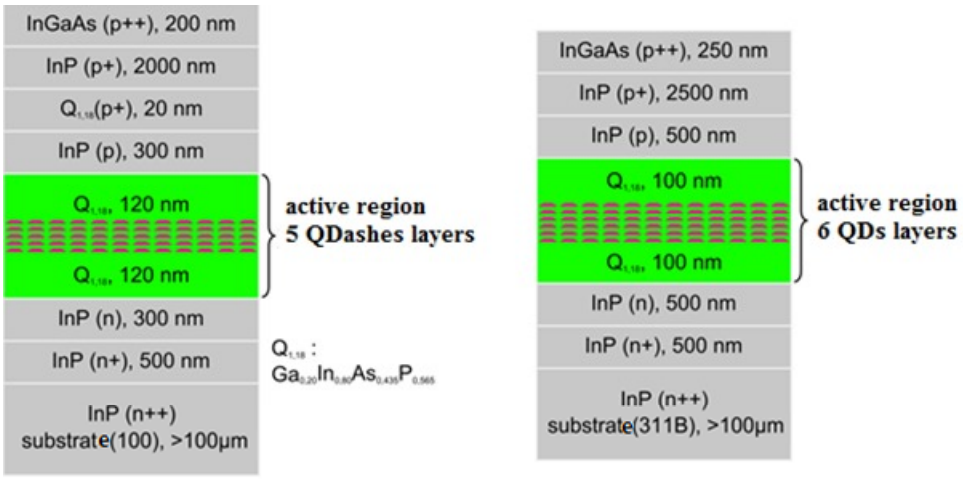


Figure 1: schematics of the epi-structures of (a) InAs/InP QDashes and (b) InAs/InP QDs SOAs

## 4. SEGMENTED CONTACT MEASUREMENTS

QD and QDash SOAs described in the previous section are used to extract both the modal gain and the optical loss characteristics based on the 4-section segmented contact method [3]. Figure 2 shows a schematic of the experimental setup monitored by the Labview friendly user interface. SOAs are mounted on a support with a Peltier-based element to control the device temperature. The electrical contacts are made with non-retractable probes powered by a current source with multiple outputs. Laser radiation is coupled into a lensed single-mode fiber as well as to a polarization controller. To prevent any optical feedback in the SOA, the use of an optical isolator in the experimental loop is required. Finally, an optical splitter is used to separate 5% of the light to monitor the alignment while 95% is sent to the optical spectrum analyzer.

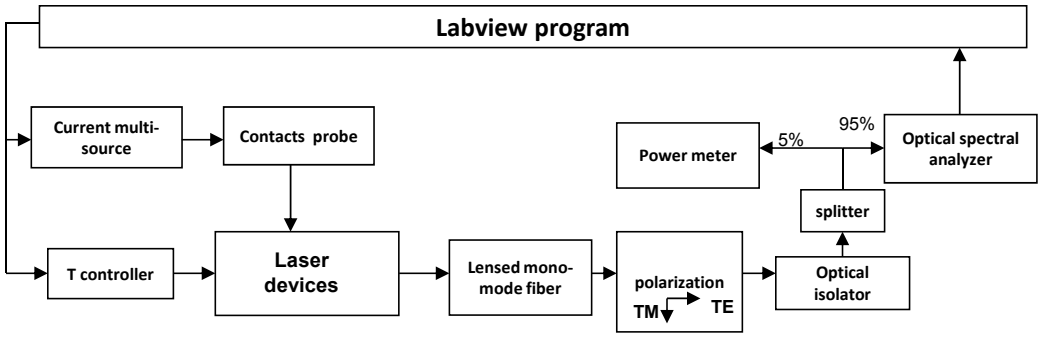


Figure 2: Schematization of the measurement setup

Figures 3 and 4 depict the measured modal gain as a function of the pump current density for both QD and QDash MLLs at 20°C and 50°C. Here, the reverse bias voltage applied on the saturable absorber section is fixed to 0 V. As expected the gain decreases at large temperature and saturates at high current density while it is red-shifted with increasing the temperature. We observe that the net gain is higher for devices made with QDashes with a maximum value of 26 $cm^{-1}$ as compared to 17 $cm^{-1}$ for QDs.

Figure 5 show the evolution of the optical loss as a function of the wavelength for various temperatures ranging from 20°C to 50°C. As shown both for QDs and QDashes, the losses curves are found to be red-shifted when increasing the temperature. The asymptotic limit of the losses curves at longer wavelength gives the internal loss coefficient whose variations are depicted in figure 6 for the two type of QNs. Typical values are found to increase from about 3 $cm^{-1}$ to 5 $cm^{-1}$ for QDs while it is enhanced from 6 $cm^{-1}$ to 12 $cm^{-1}$ for QDashes. These values are then used in the following and implemented in the analytical model to calculate the stability maps over temperature.

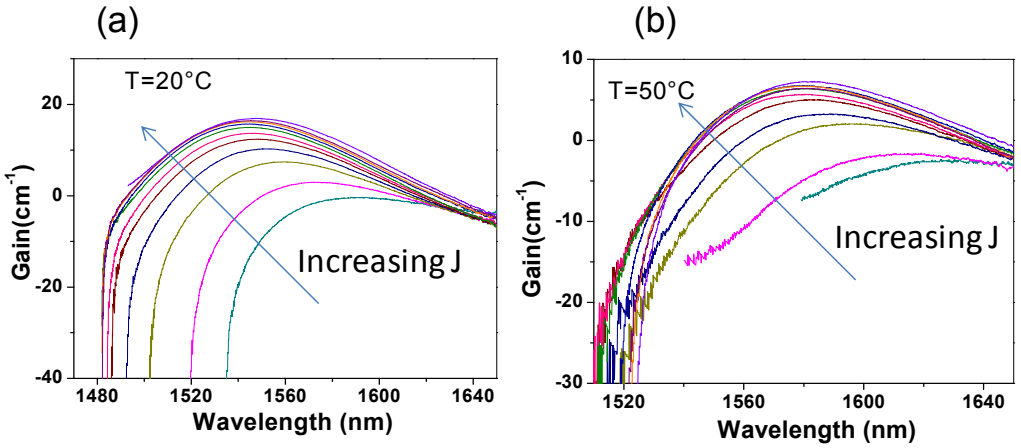


Figure 3: Measured modal gain spectra for QDs using the 4 segmented contact method for different current densities and at (a) 20°C and (b) 50°C

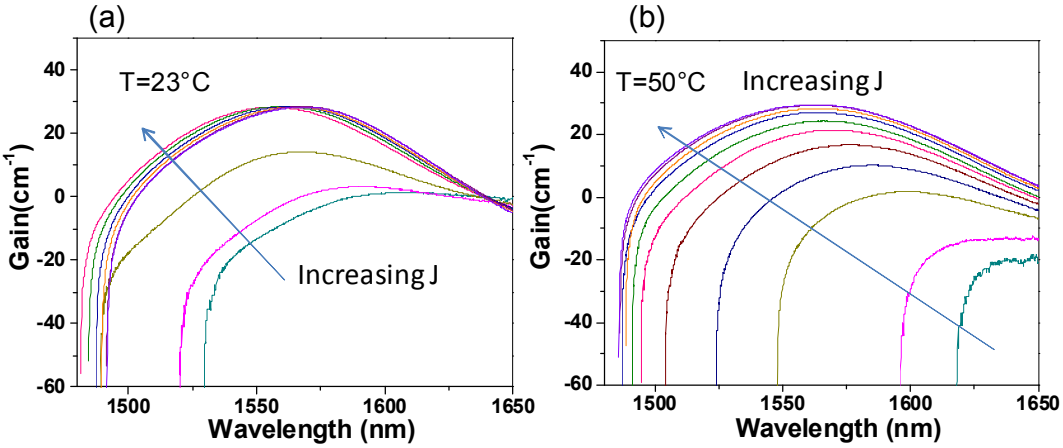


Figure 4: Measured modal gain spectra for QDashes using the 4 segmented contact method for different current densities and at (a) 23°C and (b) 50°C

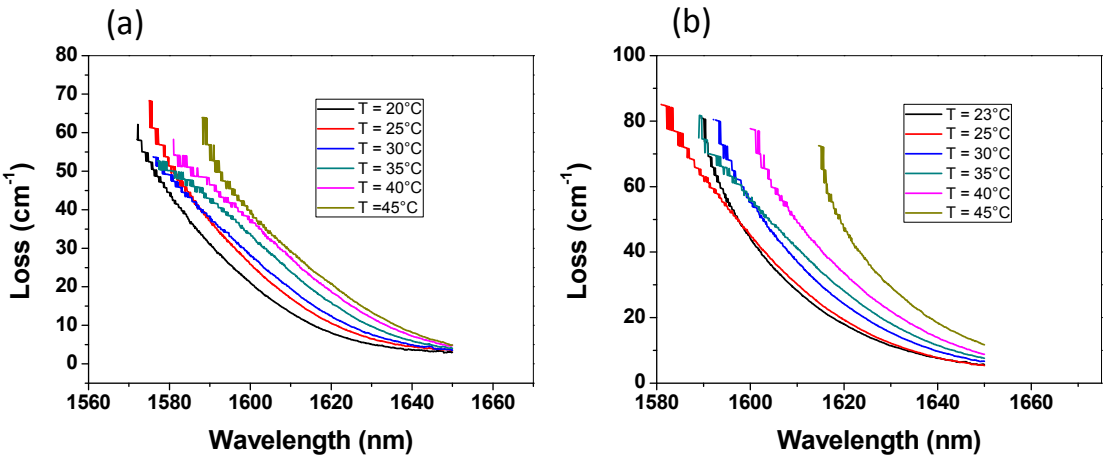


Figure 5: Measured total loss spectra for different temperature and for (a) QDs, (b) QDashes

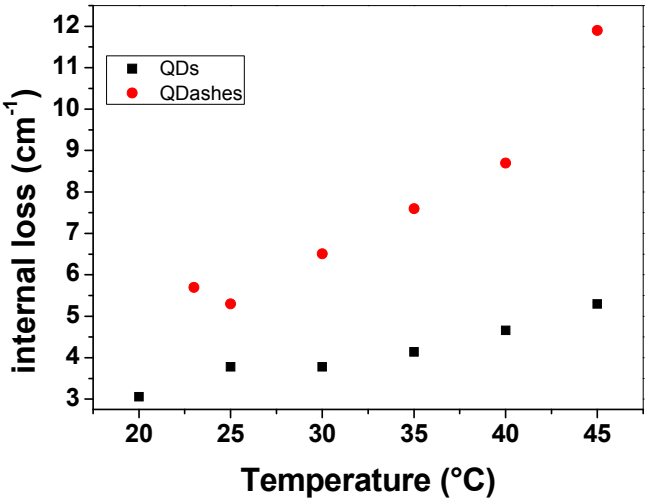


Figure 6: Measured internal losses for QDs and QDashs at different temperatures under study

## 5. RESULTS AND DISCUSSIONS

As previously mentioned, the knowledge of the loss parameters can be used to describe the variations with the pump current density of the modal gain as well as the differential gain dg/dJ whose classical expressions are given as follows,

$$g(J) = g_{\max}\left[1 - \exp\left(\frac{(J_{tr} - J)}{b}\right)\right] + \alpha_p \quad \textbf{(3)}$$

$$\frac{dg}{dJ} = \frac{g_{\max}}{b}\exp\left(\frac{J_{tr} - J}{b}\right) \quad \textbf{(4)}$$

In equations (3) and (4), $g_{max}$, $J_{tr}$ and b are adjusted to properly curve-fit the modal gain as well as to extract the differential gain with respect to the current density. Injecting (3) and (4) into (1) and (2) allows to end-up with simpler expressions. Then, equations (1) and (2) which correspond respectively to the lower and upper boundaries of the mode-locking condition can be plotted for various pump current densities. Applying this model to measurements at different

temperatures, operating maps for the mode-locked lasers under study can be extracted. Figure 7 shows the evolution of the modal gain (gain peak) for (a) QDs at 20°C and (b) QDashes at 23°C based devices. In both cases, the solid line is a curve-fitting based on equation (3). The increase of the pump current density leads to a saturation of the modal gain which occurs when the ground state level of the QN are filled. Figure 8 depicts the corresponding variation of the differential gain reported as a function of the pump current density. Because of the efficient carrier filling of the fundamental quantum level, the differential gain of the ground state level strongly decreases down to ultra-small values when the saturation is reached. This last point which leads to a high gain saturation energy is favorable to mode-locking operation as shown by equation (1). Experimental results point out that the modal gain is about twice for QDashes (30 $cm^{-1}$) as compared to the QDs (15 $cm^{-1}$). This large difference between the two types of the nanostructures is still under investigation but could be attributed to a better quality of the epi-structure obtained when growing InAs nanostructures on conventional InP(100) stubstrate.

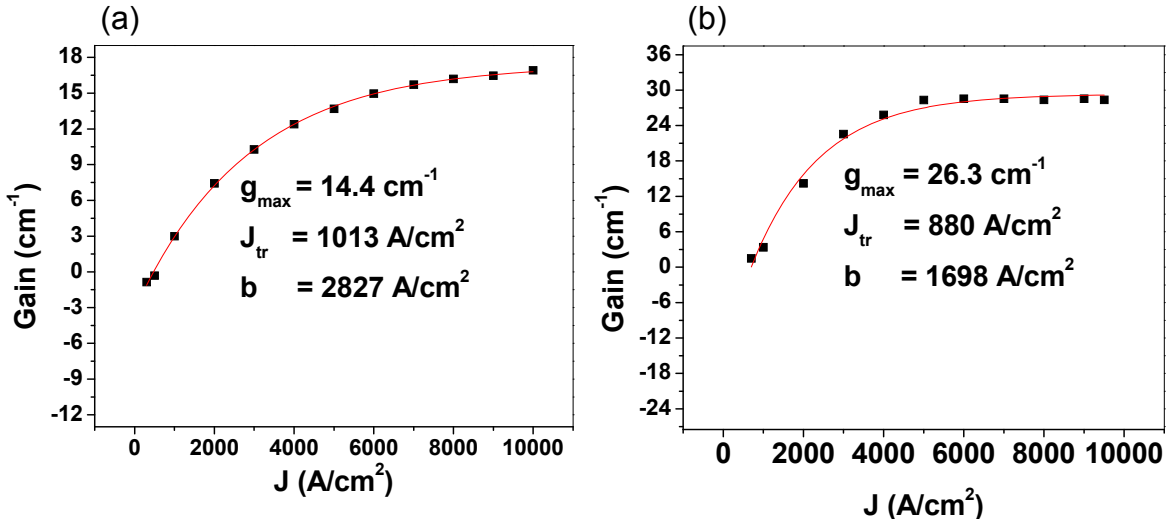


Figure 7: Measured values of the modal gain extracted from the gain peak as a function of the current density for (a) QDs at 20°C and (b) QDashes at 23°C. The red line curve presents the fit of the experimental points using equation (3)

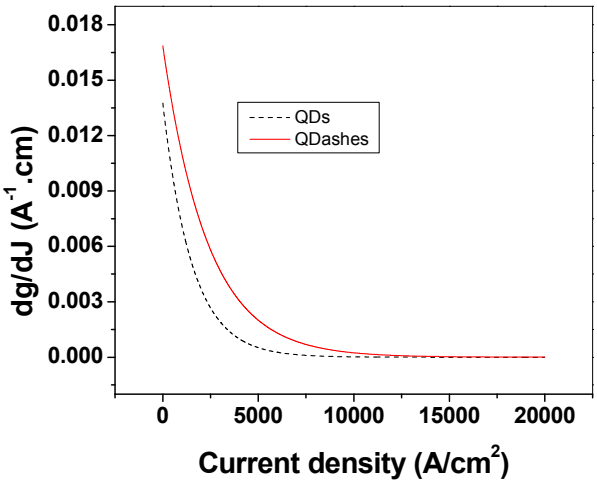


Figure 8: Differential gain dg/dJ for QDs (at 20°C) and QDashes (at 23°C) as a function of the pump current density

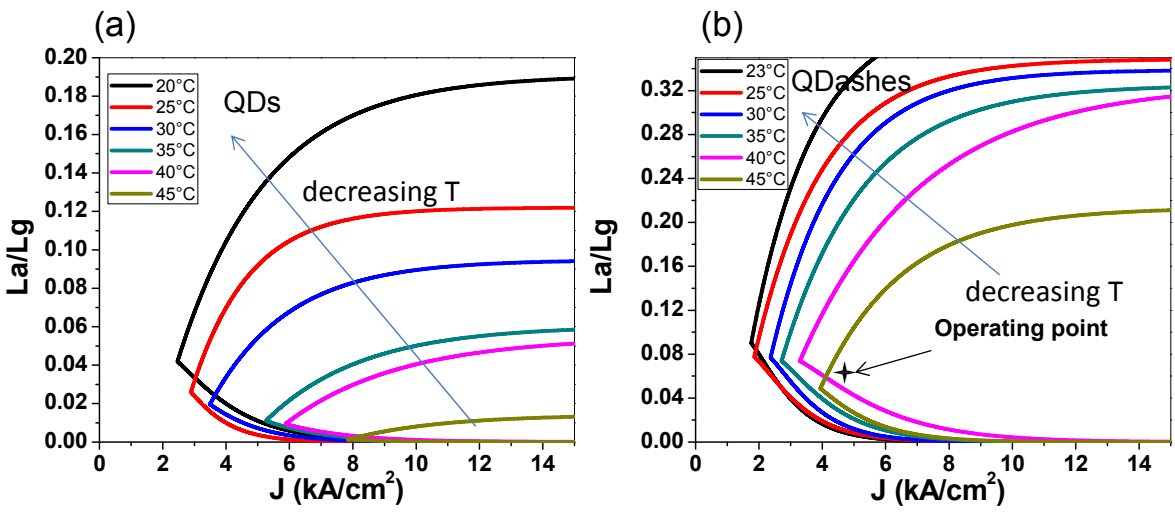


Figure 9: calculated ML stability maps for (a) QDs and (b) QDashes.

Figure 9 shows the mode locking stability map in the (La/Lg, J) plane both for (a) QDs and (b) QDashes. Various temperature conditions ranging from room temperature to 45°C are also taken into account. In the case of the QD material, simulation point out that the temperature strongly alters the mode-locking conditions. Although the first operating point at 20°C is obtained for a pump current density as low as 2.4 kA/cm$^2$ and with $L_a/L_g$=4%, it is important to note that the area of the mode locking operation is strongly shrunk when increasing temperature from 20 to 45°C. For instance, at the largest temperature, simulation shows that the mode locking takes place for a pump current density of 8 kA/cm$^{2,}$ which represents an increase by a factor of 4 as compared to the situation at room temperature. On the other hand, the area of the stability map remains extremely limited since the absorber to gain section length ratio is such as $L_a/L_g$<0.02. On the contrary, in the case of the QDash material, the temperature has a relatively low impact on the device operation. As shown in figure 9(b) mode locking is possible until 45°C with a lower pump current density of 4 kA/cm$^2$ and $L_a/L_g$=4%. Regarding the ratio $L_a/L_g$, the use of QDashes clearly provides more flexibility in maintaining a wide-opened stability map even at a large temperature. Based on our QDash device parameters, the operating point can be located in the Figure 9 (b) as shown by the black cross. This point, which corresponds to $L_a/L_g$= 6% can ensure a mode locking operation from 20 to 45° C with an injected current not exceeding 530 mA.

## 6. CONCLUSION

In conclusion, we have reported a theoretical and experimental study showing the temperature effect on the QDs and QDashes InAs/InP multi-section MLLs. Modal gain and optical losses are measured using a 4-section segmented contact method. Based on an analytical model, operating maps of mode-locking are plotted as a function of the ratio $L_a/L_g$ ratio, of the current density and of the temperature for the two types of semiconductor materials. Results demonstrate that temperature has a reduced effect on QDashes rather than on QDs. A more quantitative analysis is under study to explain the origin of such discrepancies among the two types of QNs. As a conclusion, these results proof that state-of-the-art passive MLLs can be engineered to operate within a wide range of temperature and so it is of first importance for uncooled applications such as future optical interconnects and high bit rate telecommunication systems.

Acknowledgement: This work was supported by the French National Research Agency through the project TELDOT.

## REFERENCES


[1] Ohno, T., Sato, K., Iga, R., Kondo, Y., Ito, I., Furuta, T., Yoshino, K, and Ito, H., "Recovery of 160 GHz optical clock from 160 Gbit/s data stream using mode locked laser diode" Electron. Lett., vol. 40, 265-267, (2004).

[2] Aboketaf, A., Elshaari, A., and Preble, S., "Optical time division multiplexer on silicon chip," *Opt. Exp.,* vol. 18, pp. 13529–13535, Jun. 2010.

[3] Rosales, R., Murdoch, S.G., Watts, R.T., Merghem, K., Martinez, A., Lelarge, F., Accard, A., Barry, L.P., Ramdane, A., "High performance mode locking characteristics of single section quantum dash lasers", Opt. Express, vol. 20, 8649-8657 (2012)

[4] Lu, Z.G., Liu, J.R., Poole, P.J., Jiao, Z.J., Barrios, P.J., Poitras, D., Caballero, J., Zhang, X.P., "Ultra-high repetition rate InAs/InP quantum dot mode-locked lasers, Optics Communications 284, 2323-2326 (2011)

[5] Dontabactouny, M., Piron, R., Klaime, K., Chevalier, N., Tavernier, K., Loualiche, S., Le Corre, A., Larsson , D., Rosenberg , C., Semenova , E., Yvind , K.. « 41 GHz and 10.6 GHz low threshold and low noise InAs/InP quantum dash two-section mode-locked lasers in L band » Journal of Applied Physics, 111, 023102 (2012)

[6] Fiol, G., Meuer, C., Schmeckebier, H., Arsenijevic, D., Liebich, S., Laemmlin, M., Kuntz, M., and Bimberg, D., "Quantum-dot semiconductor mode-locked lasers and amplifiers at 40 GHz," *IEEE J. Quantum Electron.*, vol. 45, no. 11, pp. 1429–1435, Nov. 2009.

[7] Xin, Y.-C., Li, Y., Martinez, A., Rotter, T. J., Su, H., Zhang, L., Gray, A. L., Luong, S., Sun, K., Zou, Z., Zilko, J., Varangis, P. M., Lester, L. F., "Optical gain and absorption of quantum dots measured using an alternative segmented contact method", IEEE-JQE, 42, 7, 725, (2006)

[8] Crowley, M.T., Murrell, D., Patel, N., Breivik, M., Lin, C., Li, Y., Fimland, B., and Lester, L., "Analytical Modeling of the temperature performance of monolithic passively mode-locked quantum dot lasers", IEEE journal of quantum electronics, vol. 47, no. 8, (2011).

[9] Lau, K. Y., "Narrow-Band Modulation of Semiconductor Lasers at Millimeter Wave Frequencies (> 100 GHz) by Mode Locking", IEEE, JQE, 26, 2, 250, (1990)

[10] Lin, C. Y., Xin, Y. C., Li, Y., Chiragh, F. L., and Lester, L. F., "Cavity design and characteristics of monolithic long-wavelength InAs/InP quantum dash passively mode-locked lasers," *Opt. Exp.*, vol. 17, no. 22, pp. 19739–19748, 2009.

[11] Paranthoen, C., Bertru, N., Dehaese, O., Le Corre, A., Loualiche, S., Lambert, B., and Patriarche, G., Appl. Phys. Lett. 78, 1751 (2001)

[12] Hinooda, S., Fréchengues, S., Lambert, B., Loualiche, S., Paillard, M., Marie, X., and Amand, T., Appl. Phys. Lett. 75, 3530, (1999)

[13] Miska, P., Even, J., Dehaese, O., Marie, X., Appl. Phys. Lett. 92, 191103 (2008)

[14] Homeyer, E., Piron, R., Grillot, F., Dehaese, O., Tavernier, K., Mace, E., Even, J., Le Corre, A. and Loualiche, S., Jpn. J. Appl Phys. 46, 6903 (2007)

[15] Zhou, D., Piron, R., Dontabactouny, M., Dehaese, O., Grillot, F., Batte, T., Tavernier, K., Even, J. and Loualiche, S., Electron. Lett. 45, 1 (2009)